International Journal of Applied
and Natural Sciences (IJANS)
ISSN(P): 2319-4014; ISSN(E): 2319-4022
Vol. 7, Issue 6, Oct - Nov 2018; 53-68

International Academy of Science,
Engineering and Technology
Connecting Researchers; Nurturing Innovations

CLUSTERING BEHAVIOUR OF END-GRAFTED POLYSTYRENE CHAINS WITH ZWITTERIONIC GROUPS: EFFECT OF MOLECULAR WEIGHT AND NUMBER OF END-GROUPS

Chiotelis Ioannis

Research Scholar, Department of Primary Education, University of Patras, Rio, Patras, Greece

ABSTRACT

In this paper, we are investigating the clustering behavior of end-grafted polystyrene chains with zwitterionic end groups. Our model system offers a unique direct look to the case of clustering behavior upon the change of solvent conditions of semi-irreversibly end-grafted chains. We measured three different types of PS chains with different architecture: one, two and three end groups. We aimed to find whether these end groups are affecting the layer of the adsorbed polymeric layer as well as the distance between two anchoring points and thus the thickness of the adsorbed polymeric layer. We measured both dry and liquid phases. In liquid phase, we used measurements depicted from SFA technique while in the dry condition we used AFM measuring mainly the formed clusters after drying. AFM allows the direct observation of clustering behavior, while AFM images analysis allows the measurement of the statistical distributions and averages of the individual sizes (laterally and vertically with respect to the substrate surface) of the aggregates and their separation distances. The results are rationalised in terms of the competition between adsorption energy of end groups and clustering/aggregation behavior of chains and shows the same behavior either by SFA and AFM techniques, presenting neither significant increase in the adsorbed amount nor significant changes in the layer thickness.

KEYWORDS: *Clustering Behaviour, Semi-Irreversibly End-Grafted Chains*

Article History

Received: *21 Aug 2018* **|** ***Revised:*** *29 Sep 2018* **|** ***Accepted:*** *16 Oct 2018*

INTRODUCTION

The theoretical and experimental approach of the behavior of end-tethered polymers has employed many researchers *[1-7]*. The thickness of the adsorbed polymer layer and the magnitude of the forces that develop when two layers interact were and are the subject of intense research. In the past, significant research was carried out in the direction of the study of linear chains grafted on surfaces either through active end groups (-Zw) or through oligomers *[1, 2, 8-16]*. The question now is whether we can increase the amount of the adsorbed polymers. A reasonable answer would perhaps be that we can achieve it by chemically tying the chains to the surface *[17-22]*. However, we are interested in increasing the adsorption and thus the thickness of the adsorbed layer by natural anchoring of the chains on the surface. For this reason, we will study polymers that bear at one end instead of just one extreme group, two and three *[23-25]*.

We believe that by increasing the end groups we will achieve an increase in the adsorbed amount and thus the thickness of the polymeric layer. With the technique of the Atomic Force Microscopy (AFM), we will measure the clusters and thus the thickness of adsorbed polymeric layers directly *[2,3].*

We will present measurements in three different molecular weights of polystyrene (PS) with only one end group, that verify the theoretical predictions and these measurements will be a benchmark for the rest of our experimental measurements. Then we will mention the theoretical predictions in case we increase the number of end groups and compare them with our own experimental results. We have measured three different polystyrene molecular weights (PS) bearing two and three end groups capable to adsorb on a surface.

Alexander and de Gennes *[5-7]* by using dimensional arguments (Scaling) managed to approximate the thickness of the polymeric layer. Let's suppose that we have chains with a polymerization degree N , adsorbed from one end while the distance between the anchoring points is: s . The chains float within a good solvent forming a layer of thickness L_0 . In case we have a sufficiently high absorption amount (high surface density) that obeys the criterion $s << R_F$ where R_F is Flory radius *[26],* then we can consider the adsorbed polymer layer as a semi-dilute solution area. The adsorbed layer is assumed to show uniform concentration density with the distance from the adsorption surface *[24].*

According to the scaling arguments of P.G. de Gennes *[6,7]* we can consider each adsorbed chain layer as consisting of connected blobs. For the inside of the blobs, we can assume that we have a semi-dilute solution. Within the blobs, we have the appearance of osmotic repulsion that tends to lengthen the polymer chain. This tendency is opposed to elastic free energy, appears due to the elongation.

Relying on the calculations of Alexander *[5]* the Helmholtz free energy f per chain can be written as sum two terms:

$$f = f_1 + f_2 \tag{1}$$

The main hypothesis in our calculations is that the distance between two adsorption points s is given (or alternatively the area per polar head (end) σ that has adsorbed is known). The term f_1 includes the interaction of the polar head of the polymer with the surface $(-C)$, as well as contributions to free energy both due to the transport movements of the chains f_{tr} as well as the interactions between the polar head f_{int} . So, we can write about f_1 :

$$f_1 = -C + f_{tr} + f_{\text{int}} \tag{2}$$

However, as mentioned the thickness of the polymer layer and the behavior of the chains is determined by balancing two opposing tendencies. One tendency tends to lengthen the chains, as the other resists this elongation. The contribution of all these interactions to Helmholtz free energy Enclosed In Term f_2 *[27]:*

$$f_2 = -\delta N / L + k_1 N (Na^3 / s^2 L)^{5/4} + f_s \tag{3}$$

In this relationship, all energy expressions are in units $K_B T$.

The first term in the equation (3) is the interaction of the monomers in the chain with the adsorption surface. This interaction is expressed through δ. This term is negligible in the case of end-tethered polymers, as then the interaction is weak (values of δ are very low *[5,27]*).Where L, is the thickness of the adsorbed layer.

The second term in the relationship (3): $k_1 N(Na^3 / s^2 L)^{5/4}$ is the expression for the repulsive energy between the blobs in the adsorbed polymeric layer as has occurred from dimensional arguments (scaling) according to Daoud and de Gennes *[28]*. Where k_1 constant and s^2 the area that occupies on the adsorption surface each chain.

Finally, the third term in the relationship (3) f_S is the elastic energy (stretching energy) of the chain. In our case, of end tethering chains, where the interaction between monomers and surface (δ) is negligible, the term of elastic energy is important. According to our hypothesis, (given adsorption density σ), the adsorbed polymer layer can be characterized as dense blobs chain of diameter ξ each one. The elastic energy of blobs chains is given from the following relationship *[5]*:

$$f_S = k_2 L^2 / (N/g)\xi^2 \tag{4}$$

With g the number of monomers containing each chain ($\xi \cong a g^{3/5}$) and $\xi \cong a\Phi^{-3/4}$. Φ is the volume fraction of the monomers in the adsorbed layer: $\Phi = \dfrac{Na^3}{s^2 L}$ and k_2 constant.

Our system will be balanced when Helmholtz free energy gets its minimum value, essentially when the osmotic pressure and the elastic energy balance between them. So, the thickness L of the polymer layer will be given by the equation of the two energies:

$$k_1 N(Na^3 / s^2 L)^{5/4} = k_2 L^2 / (N/g)\xi^2 \tag{5}$$

Since we are dealing with scaling arguments, the constants k_1 και k_2 can be ignored. If we take into consideration the relations:

$$\xi \cong a g^{3/5} \tag{6}$$

$$\xi \cong a\Phi^{-3/4} \tag{7}$$

$$\text{και } \Phi = \frac{Na^3}{s^2 L} \tag{8}$$

We end up in the relationship for the thickness:

$$L_0 \approx N s^{-2/3} a^{5/3} \tag{9}$$

We observe the dependency of length L_0 from the size of the chain N, noting that in models following scaling arguments always a unit order factor is missing from the expressions we export.

The clustering behavior of irreversibly end-grafted chains and amphiphilic diblock is common. One of the most extensively studied systems is PNIPAM-grafted polymer chains onto silica nanoparticles which were shown to exhibit an non-conventional temperature-induced double phase transition behavior [29]. The phase transition at the lower temperature is ascribed to the cluster-induced collapse of the inner region of the PNIPAM brushes, close to the silica surface, which possesses a high chain density, while the transition at higher temperature is attributed to the outer region of the PNIPAM shell where the chain density is lower. A challenging issue that has emerged lately is the formation of clusters, comprising polymer-coated magnetic nanoparticles, in response to an external trigger. These clusters are advantageous for certain potential applications as for example in high gradient magnetic separation processes in which clustering enables the facile scavenging of the particles after the adsorption process [29]. Moreover, polyampholyte Janus nanoparticles comprising acidic and basic hemispheres have shown an interesting pH-responsive behavior forming clusters at low pH-values due to the excess charge on the one hemisphere of the nanoparticles followed by aggregation and precipitation of the nanocolloids at intermediate pH-values due to charge neutralization on the particle surface [30]

In our measurements, we used an AFM apparatus. AFM is a type of scanning probe microscopy (SPM), with demonstrated resolution on the order of fractions of a nanometer, more than 1000 times better than the optical diffraction limit. The information is gathered by "feeling" or "touching" the surface with a mechanical probe. Piezoelectric elements that facilitate tiny but accurate and precise movements on (electronic) command enable precise scanning. AFM has three major abilities: force measurement, imaging, and manipulation. In force measurement, AFMs can be used to measure the forces between the probe and the sample as a function of their mutual separation. For imaging, the reaction of the probe to the forces that the sample imposes on it can be used to form an image of the three-dimensional shape (topography) of a sample surface at a high resolution. In manipulation, the forces between tip and sample can also be used to change the properties of the sample in a controlled way. Examples of this include atomic manipulation, scanning probe lithography and local stimulation of cells. Simultaneous with the acquisition of topographical images, other properties of the sample can be measured locally and displayed as an image, often with similarly high resolution.

Apart from AFM, forces between a polymeric layer of such polymers were measured by the Surface Force Apparatus (SFA). Around the end of 60s Tabor και Winterton [31] constructed a device that could directly measure the Van der Waals interactions between mica surfaces in a air or in vacuum. This device was improved by Israelachvili et al [32], [33]. The improvements had to do with the highest accuracy of measurements and the ability to have immersed mica surfaces in the liquid phase. The device of Tabor and Israelachvili the following years became a basic tool for the study of forces, especially among polymers. In recent years the interest in measuring forces with the above apparatus has been revised [34-39].

In general, the measurement of surface forces is a difficult task as very weak forces need to be measured at microscopic distances. The general concept is this: if we consider a body attached in a spring of known constant and a second body approaching the original, then when the surfaces of the bodies interact the shift (deviation) of the spring from its original position (Balance position) will be proportional to the power it receives. By measuring the displacement of the spring for various distances between the two surfaces we can extract the force-removal ratio of surfaces. The distances we are interested in are of the order of nm, while typical power values are from μN to pN, depending on the size of the particles and the nature of their interaction. This is the main idea of AFM too, so the former measurements [40] are a strong comparison criterion.

Experimental Section

Materials

Three series of *end*-functionalized polystyrenes (PS) with one, two, and three zwitterionic (Z_w) end groups and different molecular weights (M_w) were used in this study (PS-Z_w, PS-2Z_w, and PS-3Z_w, where Z_w: -N$(CH_3)_2$). The characteristics of the molecules used in this study are shown in Table 1.

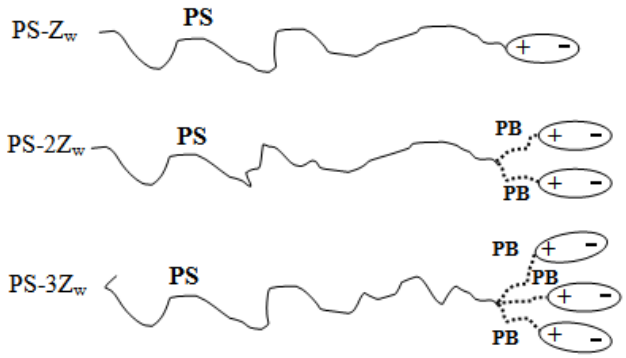

Figure 1: Schematic Representation of the Materials Investigated in this Study

Table 1

Sample	*N*	$M_n \times 10^{-3}$	$M_w \times 10^{-3}$	M_w / M_n
PS-Z_w-25	250	25	26	1.02
PS- Z_w -65	640	64	66	1.04
PS- Z_w-150	1540	154	158	1.03
PS-2Z_w-25	270	27	28	1.04
PS-2Z_w-65	650	65	67	1.03
PS-2Z_w-150	1560	156	159	1.04
PS-3Z_w-25	270	27	28	1.04
PS-3Z_w-150	1560	156	159	1.02

Sample Preparation

First, we prepare the silicon wafer substrates. We cut the silicon wafers into precise 10x10 cm plates double wash them with triple distilled water and pure alcohol solution (99,999%). Then we allow the wafer to dry under the controlled condition of the chemically inert atmosphere. We use argon or helium atmosphere. Then we prepared polymer solution 0,1-02% concentration in toluene as dilution means. We place the silicon wafers into the polymeric solutions and let them incubate for more than 12 hours, night long. We then leave the wafers bearing now the adsorbed polymeric layers to dry under controlled toluene atmosphere for a couple of hours. We are now ready to measure our samples by means of AFM.

Atomic Force Microscopy

All the AFM experiments have been performed in air (bad solvent for the PS-Z_w molecules) with a MultiMode 8-HR Atomic Force Microscope. The samples were imaged in tapping mode with a nominal spring constant of 20 Nm and a resonance frequency of 110 kHz was used to image the samples.

Island Height and Island Surface Coverage Calculations

The software Scanning Probe Image Processor (SPIP, Image Metrology) was used for simple leveling and display. The island heights and surface coverage (percentage of substrate surface covered by polymers) were determined by using either the grain analysis or the roughness analysis module (height distribution of pixels).

Surface Forces Apparatus (SFR) Experiments

From our SFA measurements, we found that the theoretical prediction $L_0 = aN^{3/5}\lambda^{2/5}$ is verified. We recall that N Is the degree of polymerization of our samples and λ is the sticking energy normalized to $K_B T$. What we tried to do is by increasing the tethering energy to measure a corresponding increase in the thickness of the adsorbed layer. However, as we see from the measurements and from the table, no substantial change was observed. This can also be seen in the graph below (Figure 2), where we represent the thickness of the polymeric layers for the three different architectures, in terms of molecular weight. Logarithmic representation of the thickness of the adsorbed polymer layer L_0 in a relationship with the molecular weight of three polymer M_W. With ■ is represented he Zw-PS, with ● the samples 2Zw-PS and with ▲ the architecture 3Zw-PS. With ——— The theoretically foreseeable behavior for the architecture Zw-PS. with ---------- the theoretically predicted behavior for architecture 2Zw-PS and with the prediction for the architecture 3Zw-PS. We see that the theoretical predictions for an increase in the adsorbed amounts are not followed by an increase in the tethering energy.

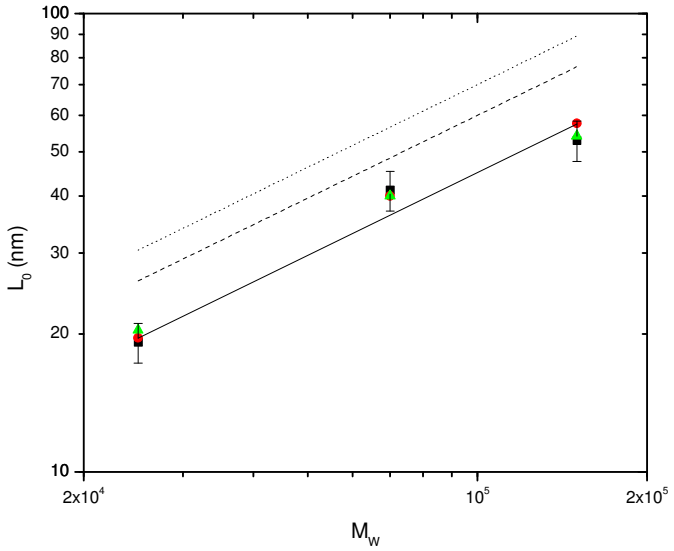

Figure 2: Thickness of the Adsorbed Polymeric Layers for the Three Different Architectures, in Terms of Molecular Weight

RESULTS

Figure **3**3 shows some typical 10 × 10 μm^2 AFM height images of all the different PS molecules used in this study (Table 1). Figure 3a, b and c correspond to the case of PS-Z_w with M_w = 26 kg/mol, M_w = 66 kg/mol and M_w = 158 kg/mol respectively. Figure 3d, e and f correspond to the case of PS-2Z_w with M_w = 27 kg/mol, M_w = 65 kg/mol and M_w = 159

kg/mol respectively. Figure 3g and h correspond to the case of PS-3Z_w with M_w = 28 kg/mol and M_w = 159 kg/mol respectively.

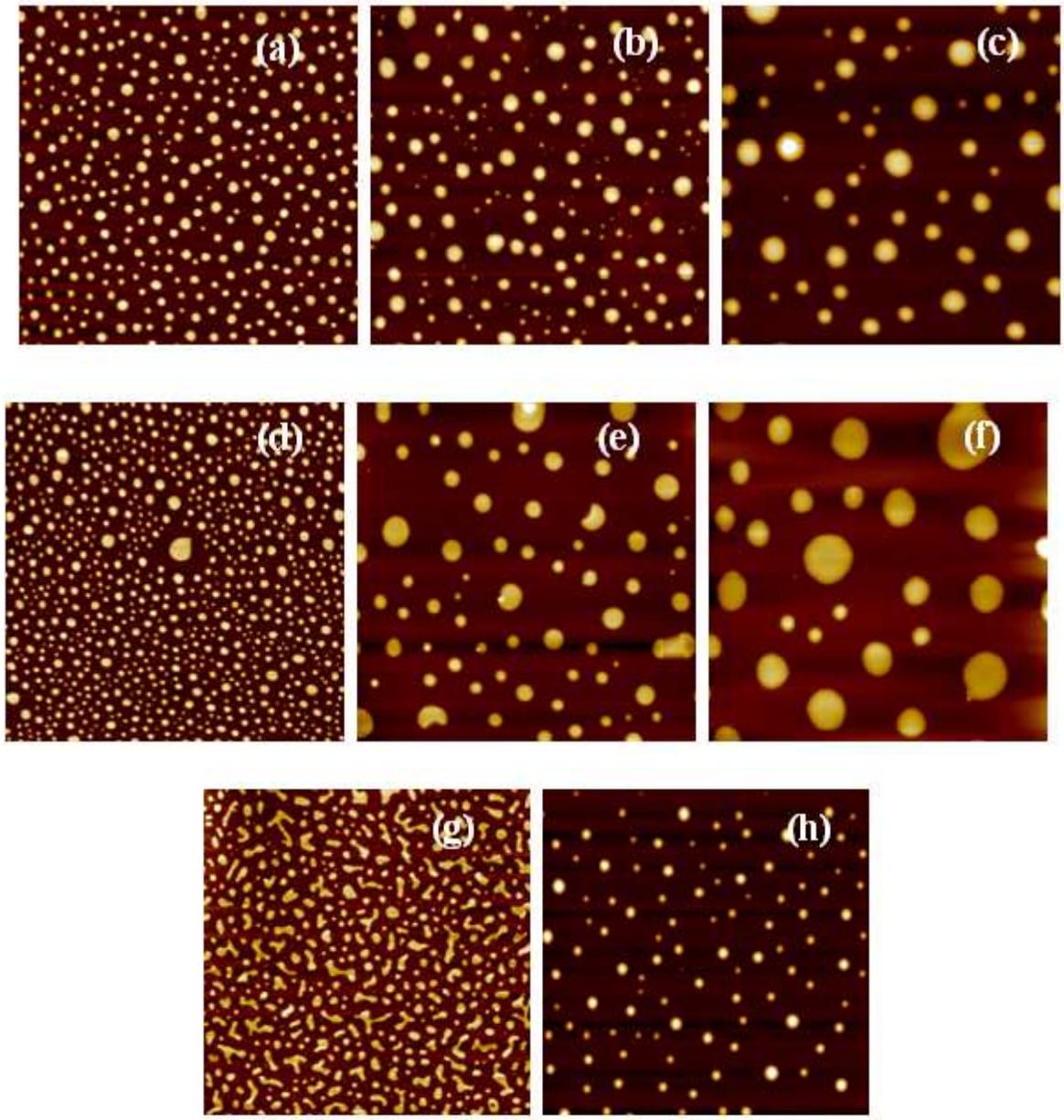

Figure 3: Typical Tapping Mode AFM Height Images (10 × 10 Mm^2) Of A Freshly Cleaned Silicon Wafer Exposed In PS-Xz_w Solutions; (A) To (C) Correspond To X=1 (PS-Z_w) With M_w = 26 Kg/Mol, M_w = 66 Kg/Mol and M_w = 158 Kg/Mol Respectively. (D) To (F) Correspond To X=2 (PS-2Z_w) With M_w = 28 Kg/Mol, M_w = 67 Kg/Mol and M_w = 159 Kg/Mol, Respectively. (G) and (H) Correspond To X=3 (PS-3Z_w) With M_w = 28 Kg/Mol and M_w = 159 Kg/Mol, Respectively

For the cases of PS-Z_w and PS-2Z_w and for all the different molecular weights used in this study the polymeric islands appeared symmetric and circular (Figure 3a to f). For PS-3Z_w with M_w = 28 kg/mol most polymeric islands took asymmetric shapes (Figure 3g) while for the higher M_w (i.e. 159 kg/mol, Figure 3h) the polymeric islands appeared again with the laterally circular shape. In all cases the polymeric islands are aggregates of several thousand polymer chains, an order of magnitude of ~10^3 to 10^4. This was calculated by dividing the number of the polymer chains per μm^2 (calculated from the corresponding adsorbed amounts) over the number of polymeric islands per μm^2 (counted from the corresponding

AFM image). These calculations are also in excellent accordance with those from SFA measurements. Analyzing AFM images for each adsorbed amount we obtained the corresponding height histograms of the polymeric islands which are shown in Figure 4. The height of the polymeric islands increased with the M_w for all the different molecules used in this study.

Table 2

Sample	Mass of a Molecule (g)	σ (mg/m^2)	Grafted Polymers Per µm^2	# of islands Per µm^2	Number of Chains Per Island
PS-Z_w-25	4.32×10^{-20}	3.16	73148	4.57	16006
PS-Z_w-65	1.10×10^{-19}	3.10	28182	2.54	11095
PS-Z_w-150	2.62×10^{-19}	2.91	11107	0.58	19150
PS-2Z_w-25	4.65×10^{-20}	3.40	73118	9.38	7795
PS-2Z_w -65	1.11×10^{-19}	2.47	22252	0.71	31340
PS-2Z_w-150	2.64×10^{-19}	2.70	10227	0.26	39334
PS-3Z_w-25	4.65×10^{-20}	2.49	53548	4.45	12033
PS-3Z_w-15	2.64×10^{-19}	1.93	7311	1.1	6646

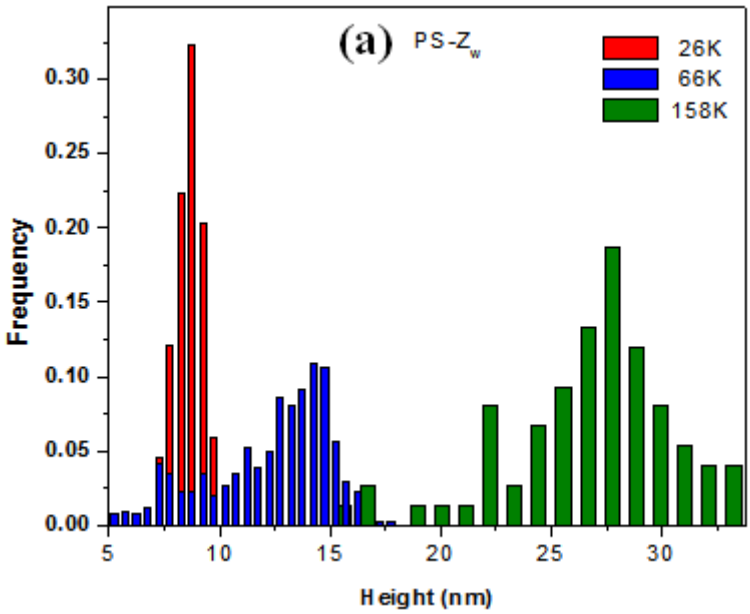

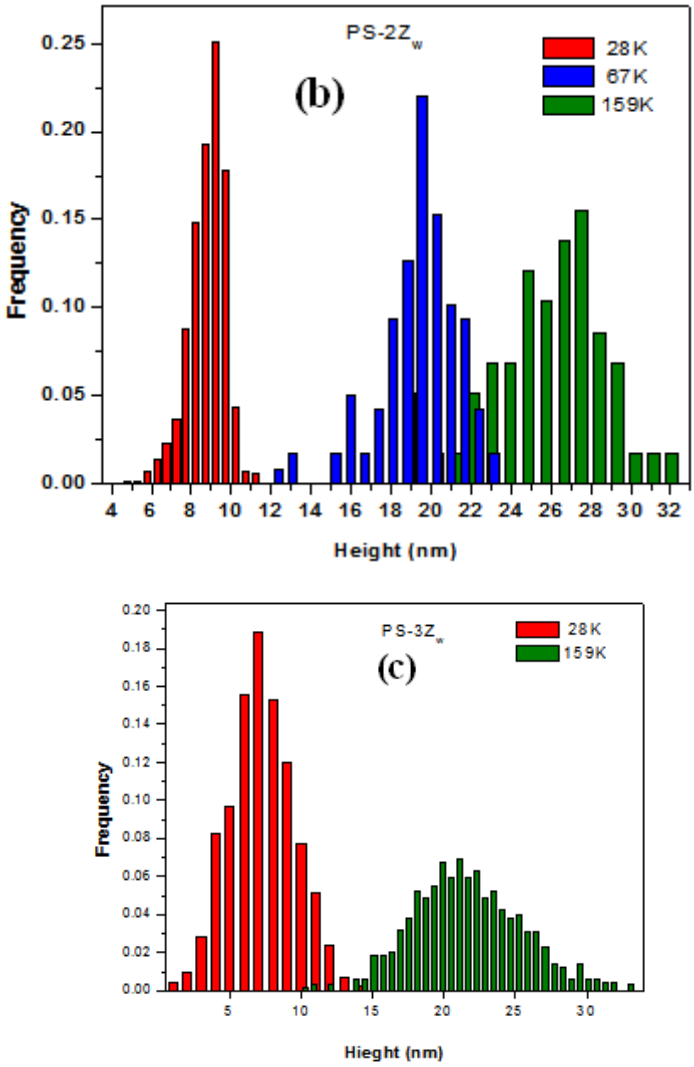

Figure 4: Total Distribution of the Islands Height Of The Polymeric Islands Appeared on the AFM Images For: (A) PS-Z_w with M_w = 26 Kg/Mol (Red Columns), M_w = 66 Kg/Mol (Blue Columns) And M_w = 158 Kg/Mol (Green Columns). (B) PS-2Z_w with M_w = 28 Kg/Mol (Red Columns), M_w = 67 Kg/Mol (Blue Columns) and M_w = 159 Kg/Mol (Green Columns) and (C) PS-3Z_w With M_w = 28 Kg/Mol (Red Columns) And M_w = 159 Kg/Mol (Green Columns)

In Figure 5 the radial average distributions of the 2D fast Fourier transform (FFT) were considered for the patterns obtained for the case of PS-Z_w with 26 kg/mol (black squares), 66 kg/mol (red circles) and 158 kg/mol (blue triangles). Generally, if the shape of an FFT is centrosymmetric implies anisotropic distribution of the pattern. The radial average distribution of a centrosymmetric shape FFT shows a clear maximum at a specific wavevector q (q=2π/λ) which corresponds to a characteristic length scale which is the preferred/characteristic distance between the polymeric islands. In all cases the 2D FFT shows a centrosymmetric shape and a clear maximum can be seen in the radial average intensity at a specified wavevector q which corresponds to a characteristic distance of 529 nm, 1.05 µm and 1.47 µm for PS-Z_w with M_w = 26 kg/mol M_w = 66 kg/mol and M_w = 158 kg/mol respectively. Centrosymetrically-shaped FFT was observed also for the cases of PS-2Zw and PS-3Z_w (results not shown). For PS-2Z_w the characteristic distances were 457 nm, 1.64 µm and 2.23 µm for M_w = 26 kg/mol, 67 kg/mol and 159 kg/mol respectively. For PS-3Z_w the characteristic distances were 519 nm and 849 nm for M_w = 28 kg/mol and 159 kg/mol respectively.

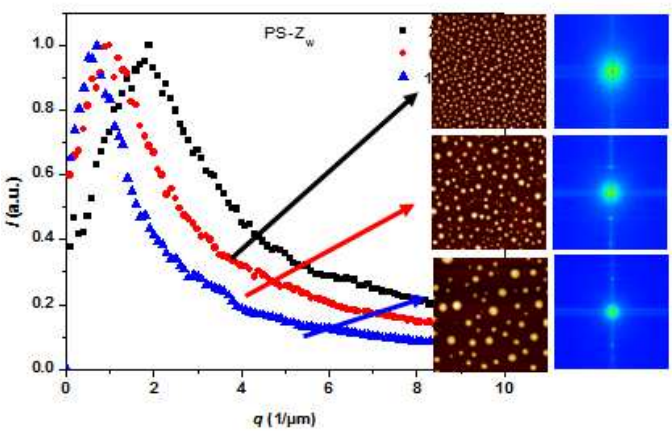

Figure 5: Relative Average Intensity (I) As A Function Of The Wave Number ($Q = 2\pi/\Lambda$) For PS- Z_w Molecules of 26 Kg/Mol (Black Squares), 66 Kg/Mol (Red Circles) And 158 Kg/Mol (Blue Triangles). These Plots Were Obtained By the Radial Average 2D FFT Image (Indicated By the Arrow, Right Image in Each Case) Resulting From The Corresponding AFM Image (Left Image In Each Case) And Show A Maximum At A Specific Wave Vector Q. By Increasing M_w the Maximum Appeared For Smaller Values of Q Which Corresponds to a Higher Characteristic Length Scale; 529 Nm, 1.05 Mm and 1.47 Mm for 26 Kg/Mol, 66 Kg/Mol And 158 Kg/Mol, Respectively

Figure 6a shows the characteristic distance of the polymeric islands, calculated from the 2D FFT image for each AFM image, against the M_w. In all case, the characteristic distance increased with the M_w. For the low M_w (≈25 kg/mol) samples the characteristic distance appears similar. Figure 6b shows the log-log plot of the polymeric islands average height versus the M_w for PS-Z_w (black squares), PS-2Z_w (red circles) and PS-3Z_w (green triangles). It is clear that in all cases the average height of the polymeric islands increases with the M_w. It is important to note that for the different molecules used in this study the average height increase following a power law with an exponent of about 3/5 (indicated with the red line in Figure 6b). For $M_w \approx 25$ kg/mol and $M_w \approx 160$ kg/mol the PS-1Z_w and PS-2Z_w appeared with similar height and higher than the PS-3Z_w. Nevertheless, for $M_w \approx 65$ Kg/mol the PS-2Z_w islands appear higher than the PS-1Z_w (Figure 6a).

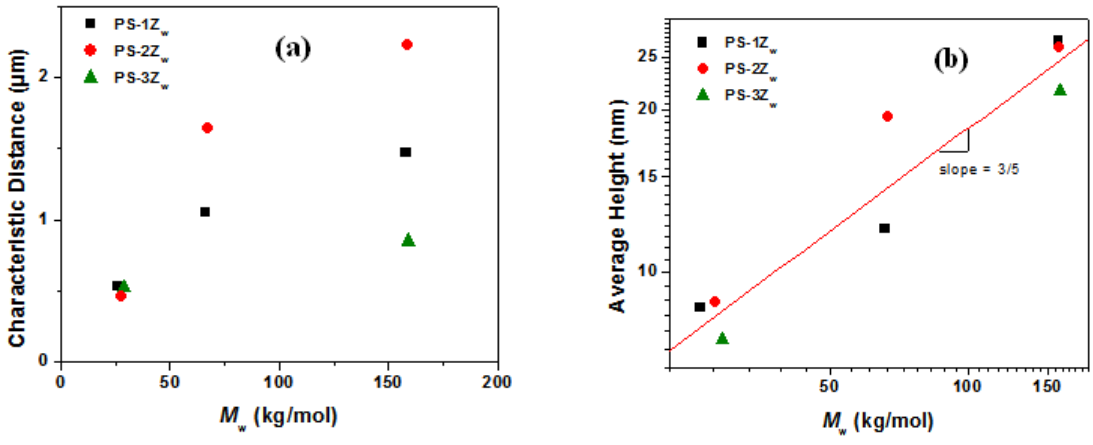

Figure 6: (A) Characteristic Distance Vs the M_w And (B) Average Height Versus the M_w For PS-1Z_w (Black Squares), PS-2Z_w (Red Circles) and PS-3Z_w (Green Triangles). in (B) the Red Line Indicates a Slope of 3/5

CONCLUSIONS DISCUSSION

Aggregation Behaviour

Our observations point to the notion that the Z_w group are not irreversibly anchored on the surface and that there is lateral mobility on the surface. Each aggregate consists of ~10^3 to 10^4 chains. This is a much higher number, 1 or 2 orders of magnitude than in the case of irreversibly anchored chains on the surface. It has been reported that thiol-terminated PS on gold surfaces, with an adsorbed amount within the brush regime, form surface micelles (aggregates) of several-ten of PS chains (i.e. ~10 to 10^2). [41-42] In this case, the lack of mobility of the anchored thiol group on the gold surface prohibits the tendency of the PS chains to aggregate together in bigger islands in order to avoid contacts with the unfavorable air and obtain more favorably energetic conformations. Consequently, in our system, the appearance of much bigger aggregates denotes the freedom of the Z_w group to move on the *xy* plane. In this way, it allows the formation of larger aggregates incorporating many PS chains and hence fewer contacts of PS monomers with the unfavorable air. Nevertheless, our results show that the extent of the chain-end mobility can be tailored to the number of the Z_w groups and the M_w of the chain.

The Mobility of the Zw groups in the xy Plane

In our theoretical analysis, we mentioned that according to the theory Alexander-de Gennes *[5-7]* the distance between two anchored polymer chains is given by the relationship $s \propto N^{3/5}$. The figure below (Figure 7) shows how s changes in relation to the molecular weight M (or N). The trend is evident in Figure 7 where we observe that with an increase in molecular weight we increase the distance between the anchorage points. This is perfectly understandable since large molecular weight polymers tend to occupy more space on the adsorption surface, effectively preventing new chains from reaching the surface. Thus, gradually increasing the molecular weight from 25K to 70 K and finally, to 150 K we notice a corresponding increasein s. The strange thing again is that according to the theoretical predictions we would expect with an increase in the adsorption groups from one to two and three we would have decreased thedistance s.

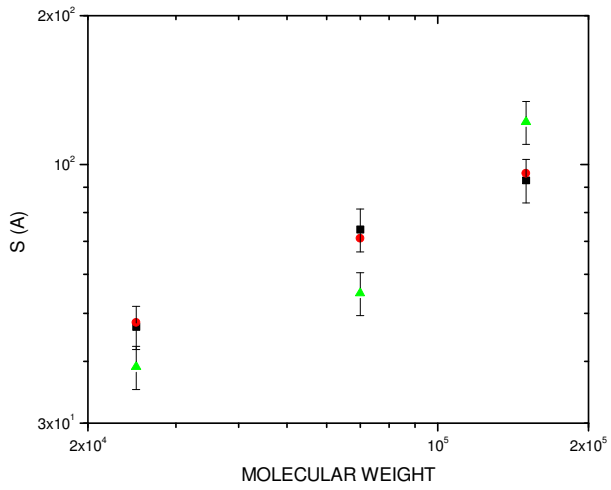

Figure 7: Logarithmic Representation of the Distance between Two Anchored Polymer Chains s in Relationship to the Molecular Weight of Polymer M_W

Effect of M_w

Figure 6a and b show that the characteristic distance and the average height of the polymeric islands increase with the M_w. Higher M_w PS chains result in higher brush monolayers due to steric repulsions, interpenetrations and entropic elasticity effects between the end-grafted chains in good-solvent conditions. When the solvent conditions change from good to bad, the longer chains can form bigger/taller aggregates and due to the increased number of entanglements the aggregates can be separated by larger characteristic distances.

Effect of the Number of the Z_w Groups

Small M_w: For the case of the small molecular weight polymers (i.e. ≈ 25 kg/mol) the samples with 1 and 2 end Z_w groups appear with a similar height while the molecules with $3Z_w$ appear shorter (Figure 6b). In addition, the AFM image for the case of the PS-$3Z_w$ with M_w = 28 kg/mol shows that the polymeric islands appear asymmetric. The high adsorption energy of the small molecular weight PS-$3Z_w$ prohibited the formation of symmetric and high islands since the energy gain associated with the formation of aggregates with a small number of PS monomers and the reduced number of entanglements cannot adequately compete with the increased adsorption energy of three Z_w. However, it must be noted that there is no large difference in the aggregation behavior between the polymers with $2Z_w$ groups and $1Z_w$ for lower molecular weights.

Intermediate M_w: For the intermediate M_w (≈ 65 kg/mol) the PS-$2Z_w$ polymeric islands appear bigger with higher characteristic distances (Figure 6a and b) than the PS-$1Z_w$. The larger attractive interactions associated with larger chains is now high enough to generate differences in the aggregation behavior. These differences should be related to differences in the end-group adsorption energy and indicate enhanced mobility of the PS-$2Z_w$ with respect to PS-$1Z_w$ showing that the PS-$2Z_w$ chains are characterized with lower adsorption energy. This is surprising since one should expect that the adsorption energy of the PS-$2Z_w$ to be double than the case of PS-$1Z_w$. A possible scenario to explain this behavior is shown in Figure 8. Interactions between the two Z_w could be responsible for neutralizing the whole of the end-group and decreasing the adsorption energy with the surface.

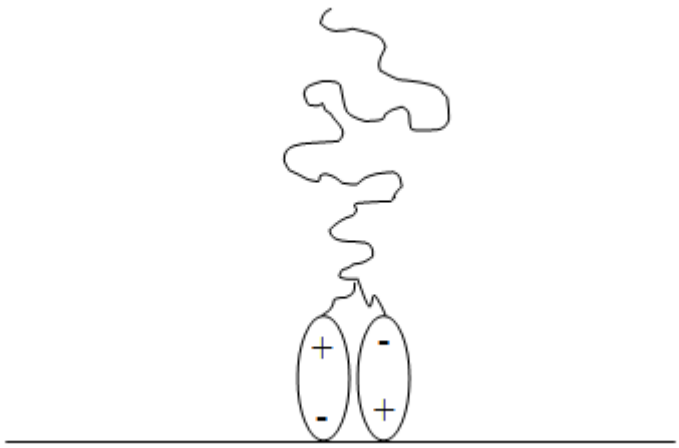

Figure 8: A Possible Scenario to Explain that Interactions between the Two Z_w Could Be Responsible for Neutralising the Whole of the End-Group and Decreasing the Adsorption Energy with the Surface

High M_w: Moving now to the case of the highest molecular weight used in this study, Figure 5 shows that the PS-1Z_w and PS-2Z_w appeared with similar height but much different characteristic distances. As it clear for the AFM images (Figure 3f) the polymeric islands for the case of PS-2Z_w are much wider (in the *xy* plane) than the case of PS-1Z_w (Figure 3c). This verifies that the PS chains with 2 Z_w groups have less adsorption energy (a scenario in Figure 8) and hence higher mobility than the case of the molecules with 1 Z_w group. For the case of PS-3Zw, the polymeric islands appear much smaller than PS-1Z_w and PS-2Z_w (in both *xy* plane and Z direction) and closer to each other indicating decreased mobility. However, the islands appear symmetric showing that the high molecular weight (~160K) results in higher forces between the PS molecules during collapsing resulting in some mobility even for the case of 3Z_w.

Comparison with Scaling Theory

A scaling theory of the clustering behavior of irreversibly end-grafted chains exists [43-44]. This is based on the difference in the surface energy between individually collapsed chains and aggregates of chains. In the case of the aggregate, the energy loss due to the stretching of anchored chains must be considered. Interestingly, this theory predicts $R \propto N^{3/5}\sigma^{1/5}$ (1), where R is the size of the core (similar to the aggregate height in our measurements), σ is the grafting density and $D \propto N^{2/5}\sigma^{-1/5}$ (2), where D is the size of the whole micelle (similar to the 'characteristic distance' between aggregates) in our measurements.

The direct application of this theory to our measurements is not possible because in our case the end-grafting is not fully irreversible (the end-group can move along the surface) and in this way, the stretching penalty can be accommodated by the direct movement of the grafted-end. However, it is interesting to note that there is a scaling type of behavior between height and molecular weight with an exponent close to 3/5. Although, this is far from being a verification of the theory for this case (grafting densities are not necessarily similar, chains are not irreversibly end-grafted, we are not sure of the importance of the stretching effect), it is an indication that a scaling-type of description can be applicable or at least we can *compare* our results to this theory and conclude indirectly if the theory's assumptions are validated by our results.

Eqs 1 and 2 predict that the product of *RD* should not depend on the grafting polymer density and scales as $RD \propto N$ (3). Figure 99 shows a log-log plot of the product of the core radius *R* (measured height from the AFM images) with the characteristic distance *D* versus the molecular weight. For the case of PS-1Z_w, the exponent is 1.19 for PS-2Z_w is 1.54 and for PS-3Z_w is 0.91. These results indicate that stretching (which signifies strong end-attachment) upon the change of solvent conditions is important for PS-3Z_w since the exponent is 0.91 (≈1). For PS-2Z_w the much larger exponent 1.54>1 indicate increased mobility of the 'grafted' end (two Z_w neutralize significantly each other) which is manifested by larger heights and characteristic distances between the aggregates as the M_w increases. The intermediate exponent of 1Z_w testifies to a behavior of intermediate mobility of the grafted end.

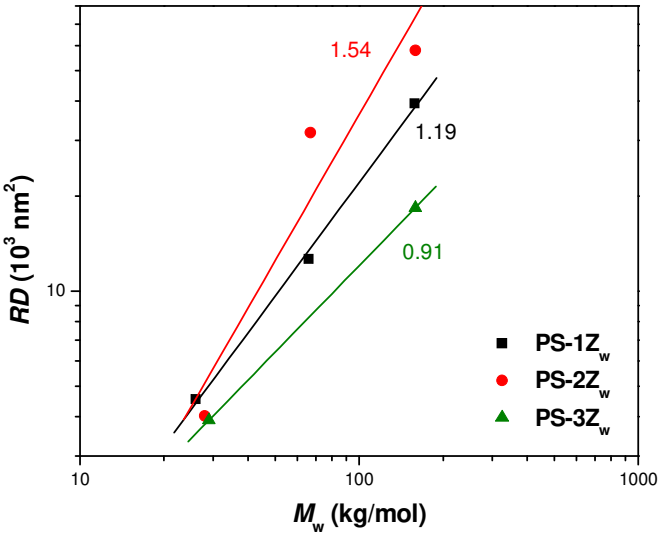

Figure 9: Log-Log Plot of the Product *RD* Versus the Molecular Weight for PS-1Z_w (Black Squares), PS-2Z_w (Red Circles) and PS-3Z_w (Green Triangles)

REFERENCES

1. *Klein, J. In Molecular conformation and Dynamics of Macromolecules in Condensed Systems, Nagasawa, M., Ed. Elsevier. Amsterdam, Holland, 1988, pp 333-352.*
2. *Taunton, H. J., Toprakcioglu, C., Fetters, L.J. & Klein, J., Nature, 332 (1988) 712.*
3. *Taunton, H. J., Toprakcioglu, C., & Klein, J., Macromolecules 21 (1988), 3333.*
4. *H. Watanabe and M. Tirrell, Macromolecules 26, 6455 (1993).*
5. *Alexander, S., J. Physics. (Paris) 38 (1977) 983.*
6. *De Gennes, P. G., C. R. Acad. Sci (Paris) 300, (1985) 839.*
7. *De Gennes, P. G., Scaling Concepts in Polymer Physics, 1985 Cornell University Press, Ithaca New York.*
8. *Homola, A. N. Robertson, A. A. J. Colloid Interface Sci. 1976 54,286.*
9. *Luckham, P.F. Klein, J. J. Colloid Interface Sci. 1987,117,149.*
10. *Hadjiioannou, G. Granick, S. Patel, S. Tirrell, M. J. Am Chem Soc. 1986,108, 2869.*
11. *Ansarifar, A. Luckham, P. F. Polymer 1988,29,329.*
12. *Taunton, H. J., Toprakcioglu, C., L J Fetters, and J. Klein. Macromolecules 1990,23 571.*
13. *B. Zhao, W. J. Brittain, Prog Polym. Sci 2000,25,677.*
14. *M. Tirrell, R. Levicky, Curr. Opin. Solid State Mat. Sci. 1997,2,668.*
15. *E.P.K. Currie, W.Norde, M. A. Cohen Stuart, Adv. Colloid Interface Sci. 2003,100,205.*

16. *J. Klein Annu. Rev. Mat. Sci.1996, 26,581.*
17. *M. Biesalski, D Johannsmann, J. Ruhe, J. Chem. Physics. 2002, 117, 4988.*
18. *S. Edmondson, V. L. Osborne, W. T. S. Huck, Chem Soc. Rev. 2004, 33,14.*
19. *K. Matyjaszewski, P.J. Miller, N. Shukla, B. Immaraporn, A. Gelman, B.B. Luokala, T. Siclovan, G. Kickelbick, T. B. Vallant, H. Hoffmann, T. Pakula, Macromolecules 1999, 32, 8716.*
20. *M. Biesalski, J Ruhe, Macromolecules 2003,36,1222.*
21. *S. T. Milner, Science 251, 905, 1991.*
22. *Halperin, M. Tirrell, and T.P. Lodge, Adv. Polym. Sci. 100,31 1992.*
23. *G. Sakellariou, S. Pispas, N. Hadjichristidis, Macromol. Chem. Phys 204,146 2003.*
24. *L. E. Dunlop, W. Briscoe, S. Titmuss, N. Hadjichristidis, and J. Klein, Macromolecular Physics and Chemistry 205 (2004) 2443.*
25. *S. Titmuss, W. Briscoe, I. E. Dunlop, G Sakellariou, N. Hadjichristidis, J. of Chemical Physics 121, 11408, 2004.*
26. *Flory, P. J. Principles of Polymer Chemistry, 1953 Cornell University Press, Ithaca New York.*
27. *De Gennes, P. G., J. Physique 37, 1976, 1445. Erratum: J. Physique 38, 1977, 426.*
28. *Daoud, M. and de Gennes, P.G., J Physique 38 1997 85.*
29. *Wu T., Zhang Y., Wang X., Liu S. Fabrication of hybrid silica nanoparticles densely grafted with thermoresponsive Poly(N-isopropylacrylamide) brushes of controlled thickness via surface-initiated atom transfer radical polymerization. Chem. Mater. 2007;20:101–109. doi: 10.1021/cm702073f.*
30. *Lattuada M., Hatton T.A. Preparation and controlled self-assembly of Janus magnetic nanoparticles. J. Am. Chem. Soc. 2007;129:12878–12889. doi: 10.1021/ja0740521*
31. *Tabor, D. & Winterton, R. H. J., Nature 219 (1968) 1120.*
32. *Israelachvili, J. N. & Adams, G. E., Nature 262 (1976) 774.*
33. *Israelachvili, J. N. & Adams, G. E., J. Chem. Soc. Faraday Trans 1, 74 (1978) 975.*
34. *L. E. Dunlop, W. Briscoe, S. Titmuss, N. Hadjichristidis, and J. Klein, Macromolecular Physics and Chemistry 205 (2004) 2443.*
35. *S. Titmus, W. Briscoe, I. E. Dunlop, G Sakellariou, N. Hadjichristidis, J. of Chemical Physics 121, 11408,2004.*
36. *Tommie W. Kelley, Phillip A. Schorr, Kristin D. Johnson, Matthew Tirrel, and C. Daniel Frisbie Macromolecules 1998 31, 4297.*
37. *M. Balastre, P. Schorr, J-F Argillier, J. Yang, J. W. Mays and M. Tirrell. In press.*
38. *M. Balastre, F. Li, P. Schorr, J. Yang, J. W. Mays, and M. Tirrell, Macromolecules 2002, 35 9480.*
39. *R. Toomey, J. Mays, J. Yang, and M. Tirrell. In press.*

40. *PhD Thesis, Chiotelis Ioannis, Investigation of interactions between absorbed polymeric layers, http://hdl.handle.net/10442/hedi/27778, DOI 10.12681/eadd/27778*
41. *Koutsos, V.; van der Vegte, E. W.; Hadziioannou, G. Macromolecules* ***1999,*** *32, (4), 1233-1236.*
42. *Koutsos, V.; vanderVegte, E. W.; Pelletier, E.; Stamouli, A.; Hadziioannou, G. Macromolecules* ***1997,*** *30, (16), 4719-4726.*
43. *Williams, D. R. M. Journal De Physique Ii* ***1993,*** *3, (9), 1313-1318.*
44. *Zhulina, E. B.; Birshtein, T. M.; Priamitsyn, V. A.; Klushin, L. I. Macromolecules* ***1995,*** *28, (25), 8612-8620.*